The Agglomeration Behaviour of
Lochiel Coal during Fluidised Bed Gasification*

D P McCullough, P J Mullinger and P J Ashman
Cooperative Research Centre for Clean Power from Lignite
School of Chemical Engineering
The University of Adelaide Adelaide, South Australia

ABSTRACT

Fluidised bed gasification (FBG) is a promising process for utilising high-sodium and high-sulphur coals, but agglomeration and defluidisation are potential problems. Experiments have been conducted to investigate these phenomena, to assist in elucidating the mechanisms at play and to develop operating solutions. It was found that agglomeration and defluidisation of Lochiel coal occur, within the 4-hour timeframe of these experiments, only when bed temperature exceeds 850°C and the air/fuel ratio is above 2.5. Agglomerates are composed mainly of silicate material, in combination with Na, Ca, Mg, Al and Fe in varying amounts. It is surmised that non-crystalline phases in agglomerates are sodium disilicate, with inclusions of Ca, Fe, Mg and Al that are expected to lower the mixture melting point, causing FBG operating problems when the total inorganic content of the bed rises above approximately 88wt% and with temperatures exceeding 850°C. It is expected that defluidisation can be avoided if operation is maintained outside of these conditions.

INTRODUCTION

Low-rank coal, or lignite, plays an important role in electricity generation in Australia. It is a desirable source of fuel, as it is relatively cheap, with the price per gigajoule of fuel approximately 20% and 10% of that for black coal and natural gas, respectively [1]. This is attributed to its relative ease of mining and its abundance, with an estimated life span of lignite reserves in Australia at over 700 years [2]. From this, it is apparent that lignite will continue to be a crucial part of electricity generation in Australia for many years to come.

Certain disadvantages exist with the use of lignite for electricity generation compared with other fuel sources. Lignite moisture content in the order of 47 to 67% [3] contribute to low thermal process efficiencies in boiler plants, while high levels of inorganic matter also exist in some lignite, particularly those from South Australia (>10% ash, dry basis [4]). Compounds of sodium, calcium, and sulphur contribute to severe fouling problems in high temperature boiler plants [5], making certain coals impractical for commercial use. These problems have driven the development of alternative methods of producing power from these coals, which may reduce or eliminate the effects of these problems altogether.

Fluidised bed gasification (FBG) is an alternative process, which provides increased efficiencies and the ability to operate at significantly lower temperatures as compared with conventional technology. It is a process involving reacting a bed of coal with an air-steam mixture generating a gas mixture primarily of carbon monoxide and hydrogen, which can be used to generate power via gas turbines. However, agglomeration and defluidisation are problems that have the potential to greatly impact on stable fluidised bed operation. These phenomena occur when ash particles within the bed become sticky at sufficiently high

temperatures, causing particle growth. When this occurs in an uncontrolled manner, fluidisation of the bed can become difficult, or even impossible. Therefore, these phenomena must be overcome prior to commercialisation of any FBG process, as they contribute to unscheduled plant downtime and increased operating cost.

Experiments have been conducted to determine the major operational influences of a fluidised bed gasification unit on the agglomeration and defluidisation behaviour of Lochiel coal, a high-sodium and high-sulphur lignite. Investigation into the inorganic species responsible for agglomeration during FBG was also carried out. From these investigations, methods for controlling agglomeration will be developed.

EXPERIMENTAL

A 77mm I.D. spouted bed gasifier (SBG) rig (10mm inlet diameter) was chosen as the fluidised bed configuration for experiments, shown in Figure 1. A spouted bed reactor consists of a cylindrical vessel with a conical base, and operates with the reactant gas passing upwards at high velocity through the centre of the coal bed, with particles circulating downwards at the walls of the vessel.
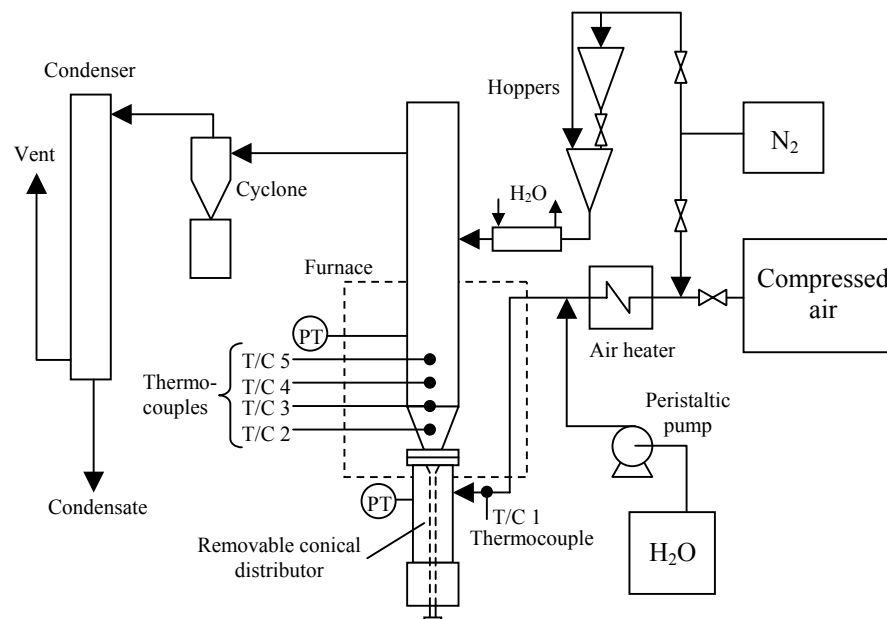

Figure 1 – Spouted bed gasifier rig

This SBG is advantageous in agglomeration and defluidisation work, as its arrangement presents the worst-case scenario to be investigated – particles at the wall of the bed are closely packed as they move down towards the base of the spout in the centre of the bed, representing a poorly fluidised bed. Also, no bed removal is performed during a run, so ash will progressively build up in the bed, potentially leading to severe agglomeration and defluidisation.

Experimental Procedure

Air-dried coal (-3.35+1.00mm particle size fraction) is fed to the hot, empty rig under a nitrogen atmosphere. The composition of Lochiel coal, and its ash, are shown in Table I and

Table II, respectively. The coal was allowed to devolatilise under the inert atmosphere conditions to produce a calculated 40 g of char before introducing air and steam. Bed temperature (thermocouples mounted along central axis, as shown in Figure 1) and pressure drop are monitored and logged at 1-second intervals during the 4-hour run. After each run, the bed is cooled down by nitrogen prior to extraction of the final bed material.

Table I – Lochiel Coal characteristics

FC (%db)	VM (%db)	Ash (%db)	Moisture		Total S (%db)	Total Na (%db)
			As-mined (%wb)	Air dried (%wb)		
38.5	47.6	13.9	59.5	12.7	3.45	0.89

Table II – Ash analysis (wt% ash)

SiO_2	Al_2O_3	Fe_2O_3	MgO	CaO	Na_2O	K_2O	TiO_2	SO_3
31.1	8.2	5.9	10.6	17.3	4.6	0.13	0.85	19.4

The experimental conditions of each run are presented in Table III. In order to maintain a constant gas velocity, while varying the air/fuel ratio, it is necessary to vary the coal feed rate, the air flow and the steam flow for each run. It is important to control the gas velocity, as well as bed temperature, since these are major factors in determining the occurrence of defluidisation [6,7].

Table III – Experimental operating conditions

Run[1]	$t_{operate}$[2] (hr)	T_{max}[3] (°C)	Air/ Fuel[4]	Steam/ Fuel[4]	Coal (kg/hr)[5]	Air rate (LPM)	Steam (g/min)	$T_{furnace}$[6] (°C)	$U_{calc.}$[7] (m/s)	$t_{defl.}$[8] (min)
2*	4.0	914	2.8	0.50	0.75	30.0	6.4	825	0.60	125
8*	4.0	885	2.8	0.39	0.88	35.2	5.8	775	0.60	170
11	4.0	826	2.8	0.50	0.92	36.5	7.7	675	0.60	-
5*	3.7	863	2.5	0.50	0.75	27.0	6.5	775	0.52	180
3	4.0	844	2.5	0.50	0.88	31.2	7.4	775	0.60	-
6	4.0	789	2.5	0.50	0.83	29.5	7.1	675	0.52	-
10	4.0	872	2.2	0.39	1.05	32.0	6.8	825	0.60	-
1	4.0	831	2.2	0.39	1.09	33.5	7.1	775	0.60	-
7	4.0	823	2.1	0.39	1.09	32.5	6.9	775	0.60	-
9	4.0	799	1.9	0.39	1.27	34.0	8.2	750	0.60	-

1 - * indicates defluidisation detected.
2 - Operating time (Run 5 stopped early owing to rapid increase of bed temperature towards end of run).
3 - Maximum measured bed temperature (average over 4-hr run time, measured at T/C 4 - see Figure 1).
4 - Mass basis.
5 - Coal feed, dry basis.
6 - Temperature of external electrical furnace around the reaction section of gasifier.
7 - Calculated velocity in cylindrical section of gasifier.
8 - Time before defluidisation detected.

Analysis

Total bed material, including any agglomerates, was collected for each run, and sieved to obtain particle size distribution, while also being tested for inorganic constitution. X-Ray Diffraction (XRD) and X-Ray Fluorescence (XRF) techniques were employed to obtain

mineralogical and elemental composition, respectively, both of the total bed material, and of the agglomerates separately. Scanning Electron Microscopy (SEM-EDAX) and Thermo-Mechanical Analysis (TMA) were also carried out on agglomerates in order to identify non-crystalline phases present.

RESULTS AND DISCUSSION

An operating map of the range of conditions investigated is shown in Figure 2. This shows that bed temperature is influenced by both air/fuel ratio and external furnace temperature, T_f (note that the external electrical furnace temperature can be varied independently of the bed temperature). From these conditions, only Runs 2, 5 and 8 showed signs of defluidisation, with large, porous agglomerates collected at the bottom of the bed in each case. Defluidisation is defined as any condition where a well-fluidised bed loses fluidisation, whether partial or total [8]. In these cases, the point of defluidisation was determined at the point where pressure drop across the bed decreased while coinciding with a sudden change in bed temperature.

The runs that showed defluidisation tendency were all above 850°C maximum bed temperature, and at air/fuel ratios of 2.5 and above. Outside these conditions, defluidisation was not observed. The reason for this air/fuel ratio dependence appears to be related to inorganic content of the bed, shown plotted against maximum average bed temperature in Figure 3. From this, it is seen that for each case where defluidisation was detected, the inorganic content is above approximately 88%, coinciding once again with bed temperatures exceeding 850°C. Outside these mutual conditions, no defluidisation occurred. However, it is possible that Run 10, with a maximum bed temperature of 872°C, may have eventually defluidised if run for longer than 4 hours – longer runs are therefore necessary to confirm whether this is the case. Further experiments are also currently being conducted, which aim to elucidate the true impact of air/fuel ratio on bed temperature, by separating its effect from external furnace temperature. These runs enable coal rate to be fixed, so a consistent bed height can be maintained throughout the experiments.
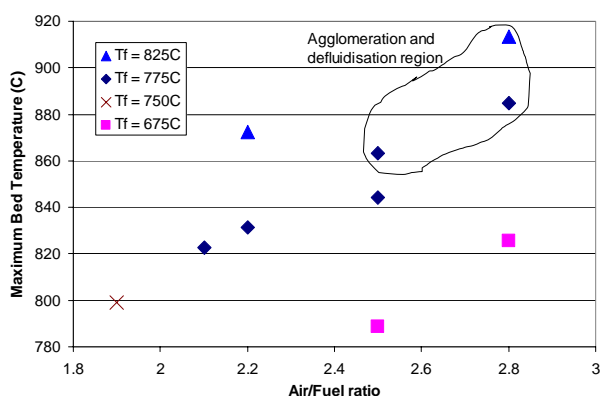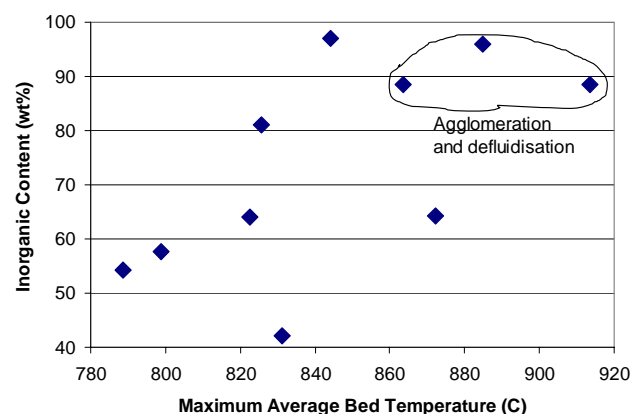

Figure 2 – Operating conditions

Figure 3 – Inorganic content vs max bed temperature

As mentioned above, bed temperature is a critical factor in determining the occurrence of defluidisation. As bed temperature is increased, the time taken for defluidisation to occur (see Table III) decreases. This trend is also reflected in the particle size distributions presented in

Figure 4. The Rosin-Rammler plot [9] of Figure 4 shows that the size distribution for the non-defluidisation runs (indicated by the curve marked 'no defluidisation') remains relatively constant, regardless of bed temperature. When defluidisation begins to occur (indicated by the 'defluidisation zone'), the curve shifts to the right. As the bed temperature increases, the curve shifts further to the right, indicating that the mass fraction of coarser particle size fractions is increasing in the bed and hence that the severity of agglomeration is increasing.

Mineralogical and elemental analyses of agglomerates from defluidisation runs are shown in Table IV and Table V, respectively. While elemental data indicates no significant difference between elemental compositions of agglomerates, mineralogical data shows a significant difference, specifically between Run 2, and Runs 5 and 8. This difference is highlighted with the appearance of sodium in the samples. Run 2 contains sodium mainly in sulphate form (thenardite) whereas in Runs 5 and 8, it is present almost exclusively in amorphous (non-crystalline) form, as evidenced by sodium comprising approximately 10% of the total agglomerate composition, yet with no significant presence in any of the other minerals detected. Based on thermodynamic calculations [10], combustion conditions are expected to result in sodium occurring only in sulphate form, whereas under reducing conditions sodium is expected to form silicates and aluminosilicates, depending on the gaseous environment and the inorganic composition of the ash. Therefore, it is expected that the sodium-containing amorphous phase in Runs 5 and 8 is a sodium silicate/aluminosilicate composition. The reason for the difference of Run 2 is unclear, and investigations are currently continuing.
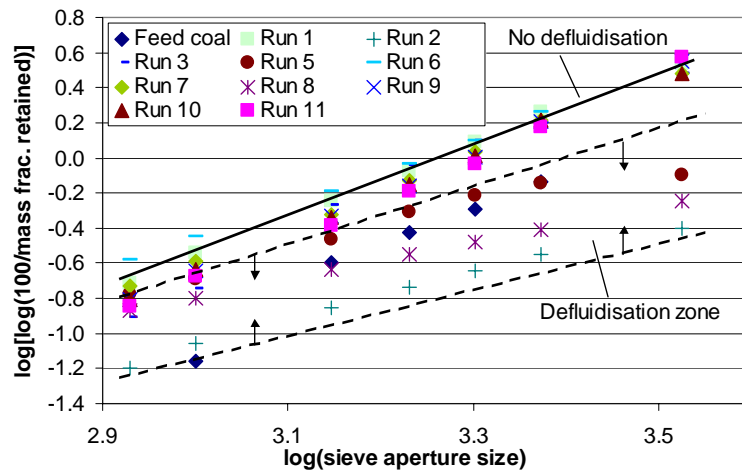

Figure 4 – Particle size distribution (Rosin-Rammler plot)

Table IV – XRD analysis of agglomerates

Run	Dominant (>60%)	Sub-dom. (20-60%)	Minor (5-20%)	Trace (<5%)
2	Gehlenite-akermanite	Augite	Quartz, monticellite, thenardite	Anhydrite, periclase, oldhamite, nepheline
5	Quartz	Gehlenite	Magnetite, augite, amorphous	Oldhamite, anhydrite, periclase, monticellite, lime
8	Quartz	Gehlenite	Augite, lime, amorphous	Oldhamite, anhydrite, periclase, magnetite, monticellite, magnesite

Table V – XRF analysis of agglomerates (wt% ash)

Run	Si	Al	Mg	Fe	Ca	Na	K	Ti	S	Total
2	38.03	7.66	10.78	8.29	18.62	12.23	0.38	1.44	2.57	100
5	43.05	5.96	8.19	7.35	17.55	13.56	0.24	1.51	2.59	100
8	41.48	6.86	9.01	5.54	21.28	11.92	0.22	1.40	2.28	100

Kosminski [11] showed that sodium disilicate ($Na_2Si_2O_5$) is the most likely sodium compound to form under gasification conditions. Sodium disilicate has a melting point temperature of 875°C in pure form [12], although this temperature is reduced at higher silicon content (789°C at 74.2 wt% SiO_2 [12]). However, other elements may also influence the melting behaviour of this compound. SEM-EDAX analysis shows that iron is enriched in several high-silicon sections of agglomerates. Many researchers have investigated agglomeration during the high temperature gasification of high-rank coal [13-16], with most coming to the conclusion that agglomeration is the result of the formation of Fe-Al-Si eutectics, with calcium, magnesium, and even sulphur playing roles in the formation of eutectic phases as well. However, the high-rank coals in these studies generally contain low sodium content, and are operated at much higher temperatures (1000-1400°C) than would be used in gasifying Lochiel coal. Hence, an Fe-Al-Si mixture in itself would not be expected to cause liquid phase formation under these relatively lower temperature conditions. However, iron addition to a $Na_2Si_2O_5$ mixture can result in melting point temperatures as low as 800°C [17]. Calcium can also cause a similar lowering of $Na_2Si_2O_5$ melting temperature, to as low as 725°C [18]. Even inclusion of aluminium to a certain extent can result in a melting temperature of 732°C [19], so it is easy to see the impact of these inclusions in a $Na_2Si_2O_5$ mixture. It is quite possible then, that the amorphous phase could be a silicate mixture containing sodium, calcium, magnesium, aluminium, and iron in various amounts, contributing to an amorphous phase that could become liquid at temperatures much lower than the melting point of pure $Na_2Si_2O_5$.

CONCLUSIONS

- For the spouting bed gasifier used in these experiments, defluidisation occurs only under specific conditions, when both temperature is above 850°C and air/fuel ratio is ≥2.5, which coincides with inorganic content of the bed >88%. While such a high inorganic content is not likely to be reached in a full-scale operation as such, these results do indicate that there exists an operating region, outside which defluidisation can be avoided.
- Under defluidisation conditions, increasing the bed temperature leads to an increase in severity of agglomeration.
- Non-crystalline phases present in the agglomerates from defluidised runs contain practically all the sodium present in the ash, and is believed to be a $Na_2Si_2O_5$ glass mixture. Evidence presented suggests that this may also contain varying levels of calcium, magnesium, aluminium, and iron, which may lower the melting point of the ash.
- More runs are being conducted to investigate the impact of longer runs on defluidisation behaviour, and also to separate the impact of air/fuel ratio on bed temperature from external furnace temperature.

REFERENCES

1. King, B., 2000, "Station systems," *Industry Induction Course*, CRC for Clean Power from Lignite, Course Notes, Ch 8.
2. AGSO, 1998, "Unpublished data"; cited in Trewin, D., 2001, "Energy and Greenhouse Gas emissions accounts, Australia: 1992-93 to 1997-98," *Australian Bureau of Statistics*, ABS Catalogue No. 4604.0.
3. Allardice, D.J., 2000, "The water in low rank coals," *Industry Induction Course*, CRC for Clean Power from Lignite, Course Notes, Ch 12.
4. Readett, D.J. and Quast, K.B., 1987, "Minerals and inorganics associated with South Australian lignites – final report," *S.A. Institute of Technology*, Report to S.E.N.R.A.C.
5. Wibberley, L.J., 1982, "Furnace deposits and corrosion," *Coal: Properties, Analysis and Effective Use*, edited by Wall, T.F., The Institute of Coal Research, University of Newcastle, 22p.
6. Siegell, J.H., 1984, "High-temperature defluidization," *Powder Technology*, <u>38</u>, 13-22.
7. Manzoori, A.R., 1990, "Role of the inorganic matter in agglomeration and defluidisation during the circulating fluid bed combustion of low-rank coals," *University of Adelaide*, PhD Thesis.
8. He, Y., 1998, "Particle agglomeration and loss of fluidisation in fluidised bed combustion," *CRC for Clean Power from Lignite*, Internal Report No. 98002.
9. Rosin, P. and Rammler, E., 1933, "The laws governing the fineness of powdered coal," *The Institute of Fuel*, <u>7</u>(31), 29-36.
10. Kosminski, A., 2000, "Reactions of sodium with silica and kaolin during gasification of low-rank coal," *CRC for Clean Power from Lignite*, Internal Report No. 00003.
11. Kosminski, A., 2001, "Reactions between sodium and silicon minerals during gasification of low-rank coal," *The University of Adelaide*, PhD Thesis.
12. Kracek, F.C., 1939, "Phase equilibrium relations in the system, Na_2SiO_3-Li_2SiO_2-SiO_2," *J. Am. Chem. Soc.*, <u>61</u>(10), 2863-2877.
13. Kolodney, M., Yerushalmi, J., Squires, A.M. and Harvey, R.D., 1976, "The behaviour of mineral matter in a fluidized bed gasifying coal–The Ignifluid process," *Trans. J. Br. Cer. Soc.*, <u>75</u>, 85-91.
14. Mason, D.M. and Patel, J.G., 1980, "Chemistry of ash agglomeration in the U-GAS® process," *Fuel Proc. Technol.*, <u>3</u>, 181-206.
15. Huffman, G.P., Huggins, F.E. and Dunmyre, G.R., 1981, "Investigation of the high-temperature behaviour of coal ash in reducing and oxidizing atmospheres," *Fuel*, <u>60</u>, 585-597.
16. Federer, J.I. and Lauf, R.J., 1985, "Crystallization behavior of coal gasification ash," *Nuclear and Chemical Waste Management*, <u>5</u>, 221-229.
17. Bowen, N.L., Schairer, J.F. and Willems, H.W.V., 1930, "The ternary system: Na_2SiO_3-Fe_2O_3-SiO_2," *Am. J. Sci.*, <u>20</u>, 405-455.
18. Morey, G.W. and Bowen, N.L., 1925, *J. Soc. Glass Technol.*, <u>9</u>, 232 and 233.
19. Schairer, J.F. and Bowen, N.L., 1947, "Melting relations in the systems Na_2O-Al_2O_3-SiO_2 and K_2O-Al_2O_3-SiO_2," *Am. J. Sci.*, <u>245</u>, 193-204.